Journal of
Materials Chemistry A

Accepted Manuscript

This is an *Accepted Manuscript*, which has been through the RSC Publishing peer review process and has been accepted for publication.

Accepted Manuscripts are published online shortly after acceptance, which is prior to technical editing, formatting and proof reading. This free service from RSC Publishing allows authors to make their results available to the community, in citable form, before publication of the edited article. This *Accepted Manuscript* will be replaced by the edited and formatted *Advance Article* as soon as this is available.

To cite this manuscript please use its permanent Digital Object Identifier (DOI®), which is identical for all formats of publication.

More information about *Accepted Manuscripts* can be found in the **Information for Authors**.

Please note that technical editing may introduce minor changes to the text and/or graphics contained in the manuscript submitted by the author(s) which may alter content, and that the standard **Terms & Conditions** and the **ethical guidelines** that apply to the journal are still applicable. In no event shall the RSC be held responsible for any errors or omissions in these *Accepted Manuscript* manuscripts or any consequences arising from the use of any information contained in them.

Journal Name

RSCPublishing

ARTICLE

A Solution-based Approach to Composite Dielectrics Films of Surface functionalized $CaCu_3Ti_4O_{12}$ and P(VDF-HFP)

Cite this: DOI: 10.1039/x0xx00000x

Received 00th January 2012,
Accepted 00th January 2012

DOI: 10.1039/x0xx00000x

www.rsc.org/

Claudia Ehrhardt,[*a] Christian Fettkenhauer,[a] Jens Glenneberg,[b] Wolfram Münchgesang,[c] Hartmut S. Leipner,[b] Martin Diestelhorst,[c] Sebastian Lemm,[c] Horst Beige[c] and Stefan G. Ebbinghaus[*a]

High permittivity $CaCu_3Ti_4O_{12}$/poly(vinylidenfluoride-*co*-hexafluoropropylene) P(VDF-HFP) nanocomposites were investigated as dielectrics for film capacitors. $CaCu_3Ti_4O_{12}$ was synthesized by two different soft-chemistry methods, namely by decomposition of a citrate precursor and a recently developed lactate precursor to identify a preferable route for nanometer scaled spherical particles with an increased interfacial area. A ball-milling step was applied to break particle agglomerates and to enhance particle distribution in the composite films. To improve the wetting of the $CaCu_3Ti_4O_{12}$ oxide particles and the polymer, a variety of surfactants, e.g. carbonic acid, silane, sulfonic acid and phosphonic acid were investigated. A successful oxide surface functionalization was achieved by 2,3,4,5,6-pentafluorobenzyl phosphonic acid, leading to stable bonds and a good structural compatibility between the surfactant and the highly fluorinated polymer matrix. The films were prepared from composite dispersions by the spin-coating technique and can be formed out of powders from both precursors, but the citrate method is preferable due to the milder synthesis conditions and the improved film homogeneity. The use of ball-milled powders as oxide component results in homogeneous particle distributions even near to the percolation threshold. In addition, such fine-grounded particles lead to homogeneous film thicknesses and decreased film roughnesses. Dielectric measurements at different frequencies revealed an enhancement of the relative permittivity by factor 5 compared to the pure polymer while the dielectric losses remained very low.

Keywords: polymer composite; calcium copper titanate; surface functionalization; dielectric properties

[*] Corresponding authors: Institute of Chemistry, Martin-Luther-University Halle-Wittenberg, Kurt-Mothes-Straße 2, D-06120 Halle (Saale), Germany.
Claudia Ehrhardt *Tel.:* +49 345 5525641; *fax:* +49 345 5527028. *E-mail:* claudia.ehrhardt@chemie.uni-halle.de;
Stefan G. Ebbinghaus *Tel.:* +49 345 5525870; *fax:* +49 345 5527028. *E-mail:* stefan.ebbinghaus@chemie.uni-halle.de

Introduction

Composite dielectrics are promising materials for technical applications such as microelectronics, capacitors and energy storage systems because they combine the good processability and high breakdown field strength of polymers with the high permittivity of oxides.[1] Recently, there has been a great interest in the perovskite-type $CaCu_3Ti_4O_{12}$ (CCTO). This relaxor-ferroelectric material exhibits giant dielectric permittivities of $\varepsilon_r \sim 10^4$ for polycrystalline ceramics and $\varepsilon_r \sim 10^5$ for single crystals. These values are almost constant in a wide range of temperatures (100–600 K) and frequencies (10^2–10^6 Hz).[2–5] The crystal structure of CCTO is cubic and centrosymmetric (space group *Im–3*) ruling out a conventional ferroelectric behaviour.[3,6,7] Several explanations for the dielectric properties of CCTO have been proposed. In the range of 100–600 K, the origin of the high dielectric permittivity was argued to be caused by both extrinsic and intrinsic factors.[8,9] The intrinsic properties are associated with the crystal structure, whereas the extrinsic factors are due to the presence of internal barrier layer capacitors (IBLC) between the semiconducting grains and surface barrier layer capacitors (SBLC).[3,5,9–12] However, the dielectric properties of CCTO are not ideal for application in capacitors because of its too high conductivity and in turn the large dielectric loss.

Besides oxides, polymers are commonly used as dielectric materials. Their advantages are a high mechanical flexibility, good processability, low cost and high dielectric strength.[13–16] In particular, highly fluorinated polymers such as polyvinylidenfluoride or copolymers thereof are known for a comparatively high permittivity of $\varepsilon_r \sim 10$ in combination with a high dielectric breakdown strength.[17,18] On the other hand, this permittivity is clearly very low compared to many oxide materials.

In summary, no single material combines all desired dielectric and mechanical properties. In contrast, composites of oxide particles embedded in polymeric organic matrices are promising candidates for high-performance dielectric materials because they can combine the high permittivity of the oxide component with the high dielectric strength and good processability of polymers.[19,20] Such composites can be solution-processed on large and flexible substrates at low temperatures and ambient pressure. Therefore, the challenge is to create a material with high permittivity and dielectric field strength without a large increase in dielectric loss, to enhance the resulting energy density.[9] In the last decade, nanocomposites became especially attractive, mainly for the large interfacial interactions, which have a significant influence on the degree of polarisation and charge separation.[21] The enhancement of surface area results in a more uniform particle distribution and an increased interfacial polarisation.[22,23] Most of the current research on CCTO–polymer composites chose the classical solid-state reaction to prepare the oxide powder.[24–28] The resulting particles are typically micrometer scaled. Until now, little is known about CCTO–polymer nanocomposites.[29–32] Various investigations focused on the effect of oxide surface functionalization to prevent particle agglomeration and to improve the particles distribution in a non-polar polymer.[19,33–36] Different agents for the oxide surface modification were investigated, including silanes, carboxylic acids, sulfonic acids or phosphonic acids.[19,30,37] Especially for $BaTiO_3$–polymer composites it was shown that the use of organophosphonates resulted in homogenous composites with improved dielectric breakdown resistances and energy storage densities.[19,33,34,38–40] Surprisingly, in case of CCTO, only investigations on the effect of surface functionalization by silanes are known.[30,37]

In this paper we report on the synthesis and dielectric properties of $CaCu_3Ti_4O_{12}$–poly(vinylidenfluoride-*co*-hexafluoropropylene) (CCTO–P(VDF-HFP)) composite films. In contrast to earlier investigations[25–32,37] a number of different approaches for the synthesis of CCTO and surface coating were used. The oxide particles were prepared by two different soft-chemistry methods, specifically by decomposition of a citrate precursor and a new lactate precursor, with the aim of yielding nanometer scaled particles for an enlarged interfacial area. The required high decomposition temperatures typically lead to particle agglomeration. Therefore, we compared two synthesis routes to identify the best method to obtain well seperated spherical particles for an inproved film homogeneity. Additionally, an extensively ball-milling step for breaking particle agglomerations is discussed. The use of small-grained ball-milled powders as oxide component is expected to result in homogeneous particle distributions even near to the percolation threshold. Another important task in generating composite films is to improve the wetting between the unpolar/hydrophobic polymer and the polar/hydrophilic oxide. This is achieved by functionalization of the oxide surface using surfactants (detergents). A stable bonding between the surfactants on the oxide is mandatory, because residual free molecules can cause an increase of dielectric loss and leakage current.[41] For this reason, the binding stability of various linkage groups comprising carbonic acid, silane, sulfonic acid and phosphonic acid was studied systematically for the first time for CCTO. Furthermore, a good chemical compatibility between the unpolar chain of the surfactant and the polymer matrix has to be ensured.[42] We obtained a successful surface functionalization with 2,3,4,5,6-pentafluorobenzyl phosphonic acid, leading to stable bonding and a good structural compatibility with the fluorinated polymer matrix. To the best of our knowledge, so far only thicker CCTO–P(VDF-HFP) composites obtained by solution casting or pressing of pellets were examined. Here, we report for the first time on thin 0-3–composite films (< 10 μm) with different oxide contents obtained by the spin-coating technique. We found that the fine-grounded nanoparticles lead to homogeneous film thicknesses and decreased surface roughnesses. Frequency-dependent dielectric measurements revealed a large enhancement of the relative permittivity compared to the pure polymer.

Experimental procedure

Material preparation

$CaCu_3Ti_4O_{12}$ (CCTO) particles were synthesized by decomposition of lactate or citrate precursors. In the recently developed lactate method (oxide denoted as L-CCTO in the following), calcium nitrate tetrahydrate (3 mmol, $Ca(NO_3)_2{\cdot}4H_2O$, >99 % Fluka) and copper nitrate hemipentahydrate (9 mmol, $Cu(NO_3)_2{\cdot}2.5H_2O$, >98 % Sigma-Aldrich) were dissolved in stoichiometric quantities in 50 ml water. This solution was mixed with a titanium(IV) bis(ammonium lactato)dihydroxide solution (12 mmol, 50 wt.% in H_2O Sigma-Aldrich) under vigorous stirring. The clear blue-colored solution was stirred continuously under heating until a viscous gel formed, which was initially decomposed at 300 °C to a black-brownish powder. This powder was grounded and finally calcinated at 800 °C in air for 12 h. The citrate precursor was synthesized according to Liu *et al.*.[43] Appropriate amounts of $Ca(NO_3)_2{\cdot}4H_2O$ (3 mmol) and $Cu(NO_3)_2{\cdot}2.5H_2O$ (9 mmol) were dissolved in 50 ml water to form solution 1. In a second beaker acetylaceton (12 mmol, >99 % Sigma-Aldrich) and freshly distilled titanium(IV) isopropoxide (12 mmol, >97 % Alfa Aesar) were mixed. After 10 minutes of stirring, an aqueous solution of citric acid (12 mmol in 20 mL water) was added and the mixture was continuously stirred for another 30 minutes. Then solution 1 was added dropwise to solution 2. Finally, ammonia solution was added dropwise until the intermediately formed precipitate was redissolved. The obtained sol was stirred under heating until a viscous gel formed. This gel was decomposed at 300 °C to a porous black-brown solid. This powder was grounded and finally calcinated at 800 °C in air for 30 minutes. The obtained oxide is denoted as C-CCTO in the following. Aliquotes of both oxide samples (L-CCTO and C-CCTO) were ball-milled with zirconium oxide balls (2 mm) in ethanol for 4 h at 300 rpm to break up particle agglomerations. A ratio powder:balls:solvent of 1:2:4 was chosen. Fine-ground powders are marked by a subscripted "*fg*" in the following (e.g. L_{fg}-CCTO for fine-ground lactate $CaCu_3Ti_4O_{12}$ or C_{fg}-CCTO for fine-ground citrate $CaCu_3Ti_4O_{12}$).

The phosphonic acid surfactants were synthesized by the Arbuzov reaction from the respective alkyl bromides (1-bromoctane 99 %, Sigma-Aldrich and 2,3,4,5,6-pentafluorobenzyl bromide >99 %, Sigma-Aldrich) and triethyl phosphite (>95 %, Fluka).[44] The obtained phosphonic esters were distilled in vacuum (150 °C, 3 mbar) to give the crude materials as colourless oils. An excess of bromotrimethylsilane (97 %, Sigma-Aldrich) was added for conversion to the corresponding silyl esters to facilitate the following hydrolysis. The final phosphonic acids, *n*-octylphosphonic acid (OPA) and 2,3,4,5,6-pentafluorobenzyl phosphonic acid (PFBPA) were yielded by hydrolysis of the silyl esters with weakly acidic hydrochloric acid (0.01 M) for 20 hours at room temperature followed by 2 hours stirring at 50 °C. The other chemicals for surface functionalization were obtained from the following sources and used without further purification: nonanoic acid (OCA, 97 %, Alfa Aesar), octyltrimethoxysilane (OMS, 96 %, Sigma-Aldrich) and 1-octanesulfonic acid sodium salt (OSA, 98 % Sigma-Aldrich).

For the surfactant surface functionalization of CCTO nanoparticles, typically 8 g powder was initially dispersed in 100 mL ethanol (96 %, analytical grade purity) for 6 hours by ultrasonication to prevent particle agglomeration. Afterwards, 3 mmol surfactant dissolved in 20 mL ethanol was added and the mixture was again ultrasonicated for 1 hour and finally stirred at room temperature overnight. Nanoparticles were separated by centrifugation and washed 3 times with excess ethanol with ultrasonication followed by centrifugation. The particles were dried for 6 hours under vacuum at 70 °C. Poly(vinylidenfluoride-*co*-hexafluoropropylene) P(VDF-HFP) (averaged M_n ~ 130 000, Sigma-Aldrich, containing 5 % HFP) was used as purchased.

Film preparation and Contacting

The composite suspensions were obtained by ball-milling of P(VDF-HFP) dissolved in *N*,*N*-dimethylformamide (DMF, analytical grade purity) together with the surface functionalized powder for typically 4 h. Films were fabricated by spin-coating of composite suspensions on aluminium-coated substrates using a Laurell Technologies Corporation spin coater WS-650MZ-23Npp/Lite with 1000 rpm for 1 min. The aluminium base electrode was prepared by thermal evaporation of 150 nm aluminium on a 24 mm x 24 mm glass substrate. After coating, the composite films were dried at 50 °C in a cabinet dryer. The film thickness was measured using a contact profilometer (Veeco Dektak 150 stylus surface profiler). Parallel-plate capacitors were prepared by deposing an array of 2 mm x 3 mm top aluminium electrodes (350 nm thickness) on the films through a mask using a thermal evaporator (Vakuumtechnik Dresden model B-30 HVT) with 1 nm/s deposition rate.

Measurements

The oxide particles were investigated by X-ray diffraction using a Bruker D8 diffractometer equipped with a silicon strip detector (LynXEye) with CuK_α radiation in the angular range 2θ = 10 – 95° applying a step size of 0.01 ° 2θ and a counting time of 0.5 s/data point. Fourier transform infrared spectra were collected on a Bruker TENSOR spectrometer with attenuated total reflectance on a diamond crystal applying a resolution of 2 cm^{-1}. Three-point BET gas physisorption measurements were done on a Quantachrome Corporation Nova 1000 using nitrogen in the range of p/p_0 0.1 – 0.3 to calculate the specific surface areas and averaged particle sizes. Thermogravimetric analysis was performed in synthetic air on a Netzsch STA 449C system (heating rate 10 K/min, Al_2O_3 crucibles, gas flow 20 mL/min). Film morphologies were investigated using an environmental scanning electron microscope (Philips ESEM XL 30 FEG). Cross-sectional SEM images were prepared by fracturing liquid-nitrogen cooled films. Frequency-dependent capacitance and loss tangent were measured with an Agilent 4284A LCR meter in the range 120 Hz to 1 MHz at room

temperature. The voltage was kept constant at 1 V. All presented dielectric properties are averaged over four parallel-plate capacitors.

Results and Discussion

Characterization of as-prepared and surfactant-coated CCTO particles

The dielectric properties of composite films are strongly influenced by particle size and shape, which can be tailored by the applied synthesis route. Two precursor routes were chosen to synthesize CCTO. Figure 1 shows the X-ray diffraction pattern obtained for the starting precursor gels, the initially decomposed solid precursors and the phase-pure CCTO powders.

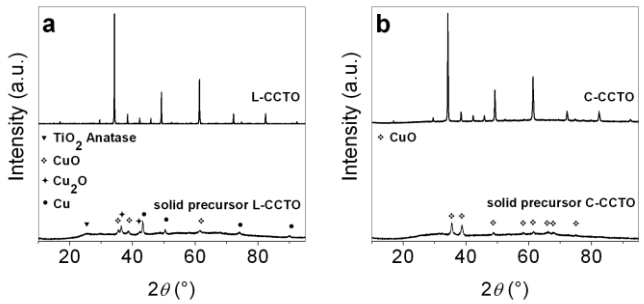

Figure 1. XRD pattern of $CaCu_3Ti_4O_{12}$ synthesized from the lactate precursor (a) and the citrate precursor (b).

Both synthesis routes lead to phase-pure CCTO (PDF card 75-2188). The starting gel of C-CCTO is amorphous, while the dried L-CCTO gel shows crystalline phases, which could not identified unambitiously. After the first decomposition step porous solid precursors were formed. In the citrate precursor only CuO was identified as crystalline phase (PDF card 48-1548), whereas the calcium and titanium components are still amorphous. The solid lactate precursor showed additionally anatase TiO_2 (PDF card 21-1272), Cu_2O (PDF card 5-667) and elementary Cu (PDF card 4-836). For this precursor, phase pure L-CCTO could only be obtained after a prolonged calcination for 12 h at 800 °C. In contrast, the citrate precursor allowed a much faster reaction of 0.5 h at 800 °C to obtain phase-pure C-CCTO. The crystallite sizes of the resulting powders were calculated with the Scherrer equation averaging the line broadenings of the main peaks (220), (400) and (422). The increased calcination time for L-CCTO caused a slightly larger crystallite size of 83 ± 3 nm compared to the value of 65 ± 2 nm observed for C-CCTO after the very short heat temperature treatment. However, both powders form porous structures due to the evolution of gaseous reaction products during the decomposition of the respective precursors. For both precursors foamy agglomerations of particles were found (Figure 2). The SEM micrographs of the powders showed particle sizes in the range of 100 – 300 nm for L-CCTO, which are slightly increased compared to C-CCTO, where particles in the range of 100 – 200 nm are characteristic. These values are slightly larger than the crystallite sizes determined by XRD measurements but in good agreement with the particle sizes calculated from BET measurements of 178 nm for L-CCTO and 146 nm for C-CCTO. The strong particle agglomeration lead us to the investigation of a further milling step to achieve a better particle distribution in the composite layers.

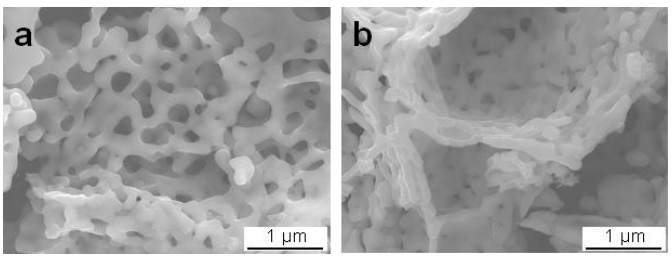

Figure 2. SEM images of L-CCTO (a) and C-CCTO (b) powders after calcination.

To improve compatibility between the oxide particles and the organic host material, the hydrophilic oxide surface was coated with surfactants. The surface modifiers should form a robust chemical bond, but it is also required to avoid residual free surfactant molecules, which can lead to a high leakage current and dielectric loss.[41] For CCTO particles, so far only the effect of silanes were investigated[30,37], while for other oxides like $BaTiO_3$ also surface coatings by carboxyl acids, sulfonic acids and phosphonic acids have been studied.[19] We therefore examined the stability of surface coating for CCTO using such classes of surfactants with the aim to generate stable and homogeneous dispersions. After surface covering, all samples were washed 3 times with excess ethanol under ultrasonication to remove non-bonded detergent molecules. The presence and binding mode of surface active molecules can be well examined by infrared spectroscopy. Figure 3 shows the C–H stretching region of FT-IR spectra for CCTO particles treated with different detergents before and after the washing step.

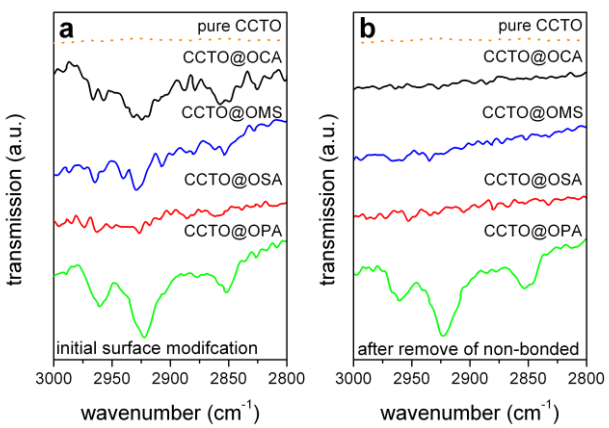

Figure 3. FT-IR spectra of CCTO particles treated with different surfactants before (a) and after removing of non-bonded surfactant by a washing step (b).

The results for C-CCTO and L-CCTO were basically identical. All depicted surfactants contain an aliphatic octyl chain with a terminal binding group, namely nonanoic acid (OCA), octyltrimethoxysilane (OMS), 1-octanesulfonic acid sodium salt (OSA) and n-octylphosphonic acid (OPA). According to

the occurance of signals in the characteristic C–H stretching region of the FT-IR spectra in Figure 3a, OCA, OMS and OPA show significant interactions with the CCTO surface. An oxide surface coating with OSA could not be observed. Figure 3b shows the corresponding IR spectra after washing 3 times with ethanol. The disappearance of the C–H stretching vibrations for CCTO@OCA and CCTO@OMS indicates that the carboxylic acid and silane molecules were only loosely adsorbed without formation of stable chemical bonds. On the other hand, the unchanged spectrum for CCTO@OPA confirms that a robust coupling to the CCTO particles is achieved by surfactants bearing the phosphonic acid group. The successful binding of the phosphonic acids is additionally proved by arising hydrophobic/lipophilic properties of the particles as shown in Figure 4.

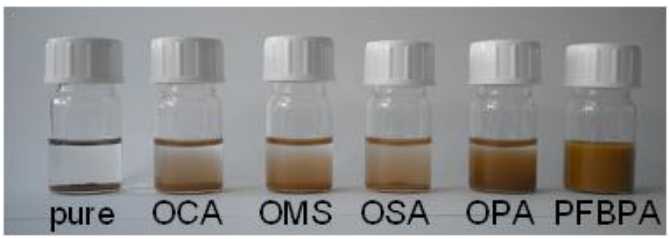

Figure 4. Photographs of dispersions in DMF of pure and various modified CCTO particles.

The surface-functionalized powders did not blend with water due to the unpolar properties of surfactants. Significant hydrophobic properties could already be observed for surfactants like OCA or OMS although no considerable coating was detected in the IR spectra. In contrast, the interaction of the various samples with the organic solvent dimethylformamid (DMF) indicates that the effect of surface coverage is highly different for the various surfactants. Especially pentafluorobenzyl phosphonic acid (PFBPA) leads to stable dispersions of CCTO particles in DMF. From the FT-IR and solvent interaction results, a good wettability with the organic polymer host can be expected for phosphonic acid-treated oxides as PFBPA provides a good chemical compatibility with P(VDF-HFP). Such a chemical similarity is expected to be mandatory for a uniform particle distribution and in turn for an increased permittivity [40]. For these reasons, only the PFBPA-treated samples are considered in the following.

The phosphonic acids can be linked to oxide surfaces in monodentate, bidentate or tridentate binding mode.[34,35] FT-IR analysis provides an insight into the binding modes of the PFBPA to the surfaces of L-CCTO and C-CCTO as well as for the fine-ground powders L_{fg}-CCTO and C_{fg}-CCTO. As shown in Figure 5 none of the uncoated CCTO samples shows any characteristic signals in the depicted region. Only the typical Ti–O stretching vibrations of CCTO were observed below 600 cm^{-1}. The pure phosphonic acid reveals broad P–OH stretching bands (around 2750 cm^{-1} and 2300 cm^{-1}), which could not be seen for the coated oxide particles verifying that these groups form bonds to the CCTO surface in at least a bidentate coupling mode.[34,35,45]

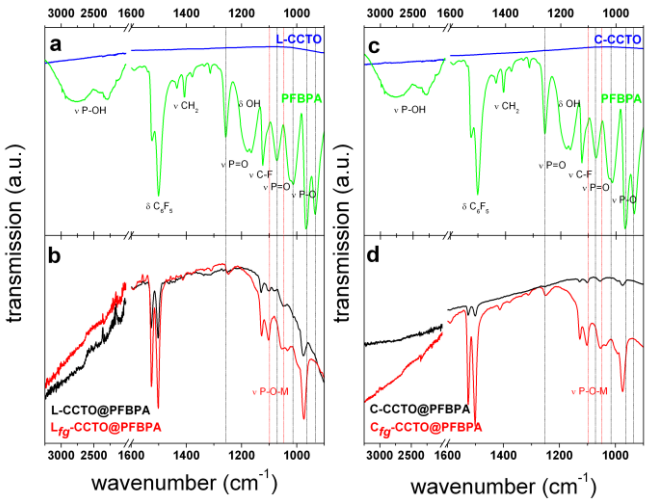

Figure 5. FT-IR spectra of pure L-CCTO and PFBPA (a), surface treated L-CCTO@PFBPA and L_{fg}-CCTO@PFBPA (b), pure C-CCTO and PFBPA(c), as well as surface treated C-CCTO@PFBPA and C_{fg}-CCTO@PFBPA (d).

After a typical surface functionalization, aromatic vibration modes (1526 cm^{-1} and 1502 cm^{-1}) and the C–F stretching mode (1126 cm^{-1}) were detected attesting the presence of PFBPA in the surface modified powders. In the finger print region between 1300 cm^{-1} and 900 cm^{-1}, major changes can be observed. Especially the P═O stretching modes (1258 cm^{-1} and 1072 cm^{-1}) and the P–O stretching modes (1020 cm^{-1}, 968 cm^{-1} and 933 cm^{-1}) of the pure PFBPA (marked by dashed black lines) turn into two main signals typical for M–O–P vibrations (M=metal; marked by dashed red lines at 1102 cm^{-1} and 1054 cm^{-1}) in case of a successful surface linking.[19,33,36,40] The changes in P═O and P–O stretching peaks of all surface modified samples indicate that the majority of surfactants is bonded to the CCTO surface in a tridentate form.

For the fine-ground powders the intensities of all peaks corresponding to the phosphonic acid are considerably increased, compared to unground powders, which reveals an enhanced surface coverage. The amount of surface-bonded phosphonic acid was quantified by gas physisorption (BET) and thermal analysis (TG/DTA). Figure 6 shows the thermogravimetry of the surface-modified powders together with the DTA signal.

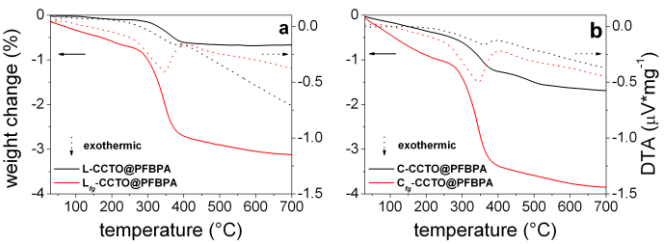

Figure 6. TG/DTA analysis of fine-ground (subscripted *fg*) and unground PFBPA surface treated powder of L-CCTO (a) and C-CCTO (b).

The first progressive weight loss below 250 °C observed for all samples most likely corresponds to residual water or remaining surface hydroxyl groups. The second rather sharp weight loss observed between 250–400 °C is assigned to the release of water, fluorine and carbon dioxide as determined by mass spectrometry.[40] This step results from the oxidative degradation of the phosphonic acid chain, while phosphorus remains in oxidic form in the sample.[40] The weight losses of both as-calcined powders are of similar magnitude, while fine-ground powders (red lines) show a much larger weight loss reflecting a higher surface area with an increased binding possibility for the surfactant molecules. The observed weight change can be correlated with the BET specific surface area of the powders to calculate the degree of phosphonic acid surface coverage Θ_{PA}, assuming a specific area of 24 Å^2 per molecule phosphonic acid.[39,46] In this calculation, the observed weight change during the exothermic reaction was interpreted as the complete combustion of the organic chain of the phosphonic acid. The average number of coupling molecules per nm^2 (*PA*) is given by

$$PA = \frac{\Delta m_{PA-chain} N_A}{M_{PA-chain} A_{spec}} \quad (1)$$

where Δm is the weight change taken from thermogravimetry, N_A is Avogadro's number, M is the molar mass of the phosphonic acid organic chain and A_{spec} the specific surface area of the modified powder. The corresponding values used for calculation of PA are listed in Table 1.

Table 1. BET surface, TG weight change, temperature interval of the combustion reaction, number of phosphonic acid molecules per nm^2 and degree of surface coverage of the modified CCTO particles.

sample	A_{spec} (BET) (m^2*g^{-1})	Δm (%)	ΔT_{wt} (°C)	PA (nm^{-2})	Θ_{PA} (%)
L-CCTO@PFBPA	7.5	0.51	250 – 400	2.2	54
L_{fg}-CCTO@PFBPA	19.3	2.00	250 – 400	3.4	83
C-CCTO@PFBPA	9.2	0.81	250 – 400	2.9	70
C_{fg}-CCTO@PFBPA	18.8	2.33	250 – 400	4.1	99

From the BET measurements it can be concluded that the grinding increases the specific surface area of both CCTO samples to roughly 19 m^2g^{-1}. As a consequence more phosphonic acid molecules can bind as revealed by the increased weight loss during the thermogravimetry of fine-ground CCTO powders. The degree of surface coverage is an appropriate measure for the achieved functionalization. Without grinding a maximum coverage of 70 % was reached only. It can be assumed that the fine porous structure of unground powders prevents the formation of a complete surfactant monolayer. In contrast, high surface coverage was obtained for the ball-milled samples. Especially for C_{fg}-CCTO@PFBPA a nearly complete surface coverage of 99 % was achieved. This very effective functionalization provides a good compatibility with the fluorinated polymer host.

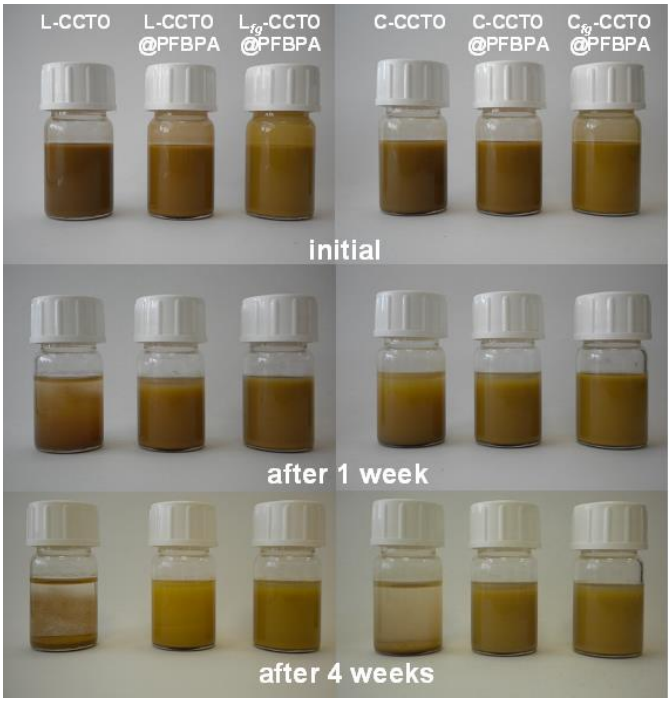

Figure 7. Photographs of suspensions of unmodified and phosphonic acid surface functionalized unground and fine-ground particles from L-CCTO and C-CCTO taken at different times.

This is evidenced by Figure 7, which shows the stability of pure and PFBPA modified CCTO dispersion in a P(VDF-HFP)/DMF polymer solution. Initially, all powders form stable composite dispersions. However, suspensions of pure CCTO already began to separate after 1 week. In contrast, the phosphonic acid treated powders form dispersions with long time stabilities. In particular for the fine-ground powders with their nearly complete surface coverage the dispersions were found to be unchanged even after 4 weeks.

Morphology and dielectric properties of composite films

After surface coverage with PFBPA, $CaCu_3Ti_4O_{12}$/P(VDF-HFP) composite films with different oxide volume contents were prepared by spin-coating of DMF suspensions. After drying, the resulting film morphologies were studied by SEM inspection of cross sections.

The particle distribution and homogeneity of the composite materials are the key parameters for enhanced dielectric properties. An oxide filling of 50 vol.% was chosen as upper limit. This content is close to the percolation threshold estimated by numerical calculations.[33,38,47] For the high content composites, the oxide particles are very densely packed preventing a clear insight into the film morphology by SEM. Therefore, composites of 30 vol.% oxide are shown for the L-CCTO@PFBPA and C-CCTO@PFBPA powders in figure 8.

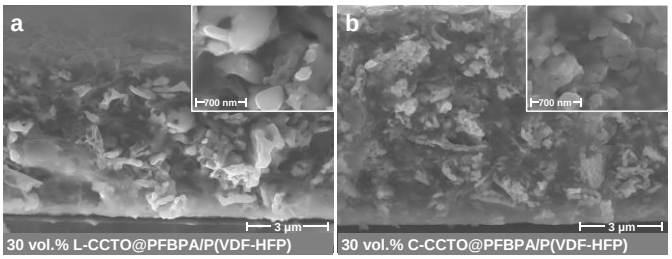

Figure 8. Cross-section SEM images of spin-coated composite films of 30 vol.% CCTO from the lactate precursor L-CCTO@PFBPA/P(VDF-HFP) (a) and the citrate precursor C-CCTO@PFBPA/P(VDF-HFP) (b). The inset images show higher magnifications.

For both as-prepared powders the particles are distributed rather inhomogeneously over the entire composite film. The smooth areas in the SEM micrographs were identified as pure polymer matrix by EDX analysis while the small bright regions are CCTO inclusions. Apparently, areas with enriched oxide contents are formed, resulting from the particle agglomeration. In contrast, the use of ball-milled powders leads to a far more homogeneous particle distribution. As an example Figure 9 shows the effect of the milling step on the particle distribution in composite films with 10 vol.% C-CCTO@PFBPA (a) in comparison to films that consist of fine-ground C_{fg}-CCTO@PFBPA (b).

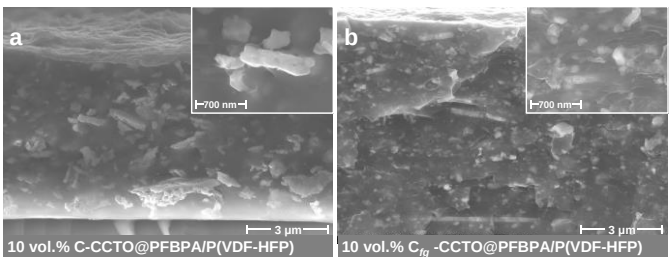

Figure 9. Cross-section SEM images of spin-coated C-CCTO@PFBPA/P(VDF-HFP) composite films with 10 vol.% C-CCTO unground powder (a) and fine-ground C_{fg}-CCTO powder (b). The inset images show higher magnifications.

For the fine-ground oxides from both the lactate and citrate precursor the nanoparticles are well separated from each other and are uniformly distributed in the composite layer. In addition, we found that the films show good mechanical properties. Composite films of fine-ground powders can be removed from the substrate after cooling with liquid-nitrogen. The obtained foils are highly flexible and can be furled even for the highest oxide contents of 50 vol.%.

As already discussed above, the milling results in a strong increase of the specific surface area and an almost complete coverage of the oxide particles by the phosphonic acid (Table 1). These isolated coated particles lead to a good compatibility between CCTO and polymer matrix, and in turn to very homogeneous films. This result is corroborated by the fact that the fine-ground particles cause a significantly decreased film roughness as shown in Figure 10.

As can be seen from Figure 10, for both precursors the fine-ground powders generate very similar film thicknesses for all oxide contents. The values are slightly smaller compared to films from unground CCTO samples. For the films based on fine-ground powders small surface roughnesses of < 0.2 µm (approximately 3 % of the thickness) were observed, which confirms the good film homogeneity.

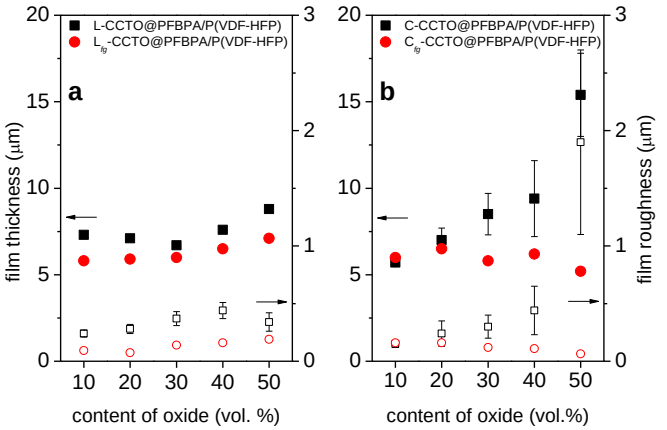

Figure 10. Film thickness (full symbols) and roughness (open symbols) of spin-coated composite films of L-CCTO@PFBPA/P(VDF-HFP) (a) and C-CCTO@PFBPA/P(VDF-HFP) (b) based on unground and ball-milled fine-ground (subscripted *fg*) powders with varying oxide volume fractions. Not depicted error bars are smaller than the size of the respective symbols.

Interestingly, composites films based on the unground oxide from the lactate precursor (L-CCTO@PFBPA/P(VDF-HFP)) show comparable thicknesses to the ones for the fine-ground material. In addition, also their surface roughnesses of approximately 0.2 – 0.5 µm (≈ 5 %) were rather small. This finding can be explained assuming that for the L-CCTO powder the ball-milling step during the composite preparation (i.e. the ball-milling of the P(VDF-HFP)/DMF solution together with the surface functionalized powder) is sufficient to break up the particle agglomerates. In contrast, composite films of unground C-CCTO@PFBPA/P(VDF-HFP) show an increasing film thickness with rising oxide volume fraction and in addition an increased roughness. Especially the 50 vol.% C-CCTO@PFBPA/P(VDF-HFP) film had a large thickness of approximately 15.5 µm and a roughness of 2.4 µm, which is about 15 %. Obviously, for the CCTO from the citrate precursor, the agglomerates are too firm to be destroyed during the milling with the P(VDF-HFP)/DMF solution. This result indicates a better processability of 0-3–composites consisting of L-CCTO.

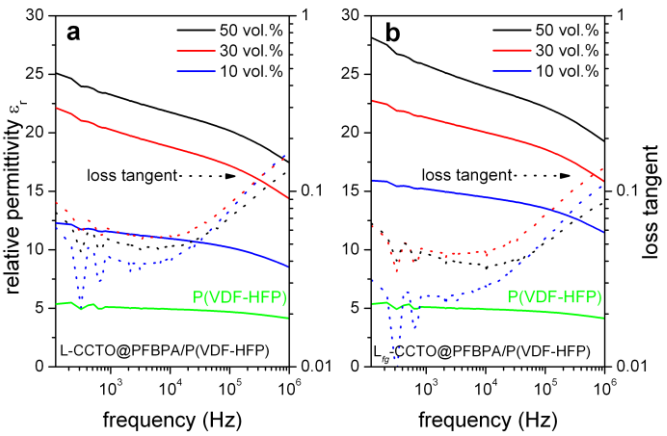

Figure 11. Relative permittivity and loss tangent of spin-coated composite films based on unground powder L-CCTO (a) and fine-ground powder L_{fg}-CCTO (b) after surface coating with PFBPA.

The good film quality for L-CCTO@PFBPA/P(VDF-HFP) samples is supported by the dielectric measurements discussed below, where increased permittivities were observed (Figure 11). For the composite films from both the as-prepared and fine-ground L-CCTO the relative permittivities ε_r strongly increase with rising oxide content. For the L_{fg}-CCTO@PFBPA/P(VDF-HFP) composite system out of fine-ground powder this effect is slightly larger. For all films the loss tangents remain low (< 0.1). For the 50 vol.% L-CCTO composites permittivities are enhanced by a factor 5 compared to the pure polymer. These findings underline the positive effect of film homogeneity on the resulting dielectric performance. In turn, the inhomogeneities in film thickness and roughness for the C-CCTO samples result in larger differences in the dielectric properties as presented in Figure 12.

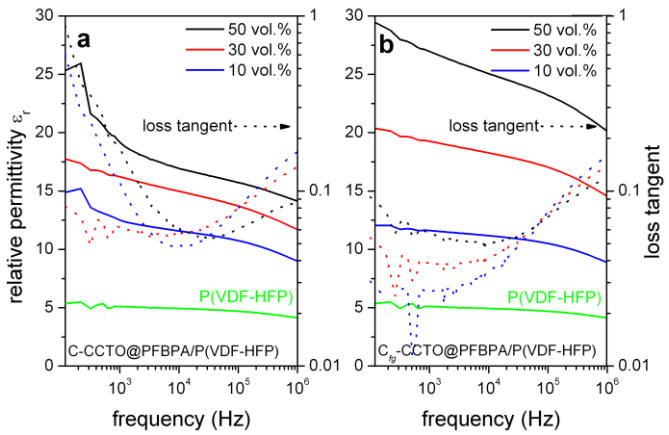

Figure 12. Relative permittivity and loss tangent of spin-coated composite films based on unground powder C-CCTO (a) and fine-ground powder C_{fg}-CCTO (b).

Composite films of both the unground and fine-ground C-CCTO also show an increase of the relative permittivities ε_r with rising oxide content similar to the L-CCTO composite films. Nevertheless, there are bigger differences between unground and fine-ground powders. For the C_{fg}-CCTO@PFBPA/P(VDF-HFP) composite system the permittivity is clearly improved compared to the unground powder while the loss tangent again remains low. For the 50 vol.% C_{fg}-CCTO composites an enhancement of permittivity by a factor 5 compared to the pure polymer could also be obtained. In contrast, the unground C-CCTO particles exhibit obviously smaller permittivities in addition to increased dielectric losses. For a 50 vol.% C-CCTO composite at 1 kHz an enhancement of ε_r to roughly 19 was found while the composite from the fine-ground oxide resulted in a value of 27. It is likely that the high deviation in film thicknesses and the increased surface roughnesses of these samples are responsible for the low dielectric performance. Therefore, our results clearly demonstrate the positive effect of grinding in the case of highly agglomerated particles. Earlier investigations on composites consisting of CCTO within a PVDF polymer host focused on thicker layers of approximately 50 – 80 µm prepared by solution casting and hot pressing. These samples showed relative permittivities ε_r up to 240 but also enhanced dielectric losses of 0.2 or higher.[27,32,48] Here, we have investigated for the first time much thinner (< 10 µm) composite films from functionalized CCTO within a fluorinated polymer matrix. These films possess relative permittivities exceeding 27 and a very low loss tangent < 0.1 at 1 kHz and room temperature. Such films can be of great interest with respect to miniaturization and multilayer applications.

Conclusions

High-quality composite films of $CaCu_3Ti_4O_{12}$/poly(vinyliden-fluoride-*co*-hexafluoropropylene) were prepared for the first time using a simple solution spin-coating technique. The oxide CCTO was synthesized by two different soft-chemistry methods, namely the already established citrate precursor route and a recently developed lactate precursor approach. After calcination at 800 °C phase-pure CCTO with a porous structure of highly agglomerated particles was obtained for both synthesis routes. To break these agglomerates a milling step was examined and found to result in improved composites properties. After milling the specific surface areas increased to roughly 19 m^2g^{-1} for both oxide powders. In order to improve the wetting between oxide surface and polymer host the binding of a variety of surfactants, namely carbonic acids, silanes, sulfonic acids and phosphonic acids to the $CaCu_3Ti_4O_{12}$ particles were investigated. While earlier reports only studied the effect of silanes as surfactants, we found that phosphonic acids form a robust surface coverage on CCTO particles. A good structural compatibility between the surfactant and the high fluorinated polymer matrix was achieved using 2,3,4,5,6-pentafluorobenzyl phosphonic acid (PFBPA) for surface functionalization. Especially with fine-ground powders a nearly complete surface coverage was obtained leading to long-time stable composite suspensions. From these suspensions composite films with oxide contents up to 50 vol.% were prepared by spin coating. Fine-ground particles lead to better composite film homogeneities as demonstrated by constant film thicknesses and decreased surface roughnesses.

The permittivities of CCTO@PFBPA/P(VDF-HFP) composite films strongly increase with rising oxide content. For fine-ground powders this effect is stronger than for the unground oxides. Both fine-ground CCTO powders (L_{fg}-CCTO and C_{fg}-CCTO) show enhanced permittivities by factor 5 compared to the pure polymer while their loss tangents remain low (< 0.1). A particularly high permittivity of 26 ±1 at 1 kHz was obtained for the composites containing 50 vol.% $CaCu_3Ti_4O_{12}$. A further increase of ε_r was revealed for these films at low frequencies while the loss tangents remained smaller than 0.1. To the best of our knowledge, so far only significantly thicker films or disks of CCTO/P(VDF-HFP) composites prepared by solution casting or pressing have been investigated. The easy processability using the simple solution-based coating technique introduced in this work leads to films with good dielectric properties making these composites promising

candidates for film capacitor, e.g. in embedded applications or as multilayer capacitors for electrical energy storage.

Acknowledgements

The work was supported by the Federal Ministry for Education and Research (BMBF) within the ForMaT/SuperKon project. Additional thanks are due to the German Federal Environmental Foundation (DBU) for financial support of a PhD scholarship.

Notes and references

[a] Institute of Chemistry, Martin-Luther-University Halle-Wittenberg, Kurt-Mothes-Straße 2, D-06120 Halle (Saale), Germany.

[b] Interdisciplinary Centre of Materials Science, Martin-Luther-University Halle-Wittenberg, Heinrich-Damerow-Straße 4, D-06120 Halle (Saale), Germany.

[c] Institute of Physics, Martin-Luther-University Halle-Wittenberg, Von-Danckelmann-Platz 3, D-06120 Halle (Saale), Germany.

1 Z.-M. Dang, J.-K. Yuan, J.-W. Zha, T. Zhou, S.-T. Li, and G.-H. Hu, *Prog. Mater. Sci.*, 2012, **57**, 660–723.

2 A. Ramirez, M. Subramanian, M. Gardel, G. Blumberg, D. Li, T. Vogt, and S. Shapiro, *Solid State Commun.*, 2000, **115**, 217–220.

3. M. A. Subramanian, D. Li, N. Duan, B. A. Reisner, and A. W. Sleight, *J. Solid State Chem.*, 2000, **151**, 323–325.

4 C. C. Homes, *Science*, 2001, **293**, 673–676.

5 P. Lunkenheimer, R. Fichtl, S. Ebbinghaus, and A. Loidl, *Phys. Rev. B*, 2004, **70**, 172102.

6 B. Bochu, M. N. Deschizeaux, J. C. Joubert, A. Collomb, J. Chenavas, and M. Marezio, *J. Solid State Chem.*, 1979, **29**, 291–298.

7 L. He, J. B. Neaton, M. H. Cohen, D. Vanderbilt, and C. C. Homes, *Phys. Rev. B*, 2002, **65**, 214112.

8 L. Ni and X. M. Chen, *Appl. Phys. Lett.*, 2007, **91**, 122905.

9 P. Barber, S. Balasubramanian, Y. Anguchamy, S. Gong, A. Wibowo, H. Gao, H. J. Ploehn, and H.-C. zur Loye, *Materials*, 2009, **2**, 1697–1733.

10 D. C. Sinclair, T. B. Adams, F. D. Morrison, and A. R. West, *Appl. Phys. Lett.*, 2002, **80**, 2153–2155.

11 A. N. Vasil'ev and O. S. Volkova, *Low Temp. Phys.*, 2007, **33**, 895–914.

12 P. Lunkenheimer, S. Krohns, S. Riegg, S. G. Ebbinghaus, A. Reller, and A. Loidl, *Eur. Phys. J. Spec. Top.*, 2009, **180**, 61–89.

13 F. Guan, J. Pan, J. Wang, Q. Wang, and L. Zhu, *Macromolecules*, 2010, **43**, 384–392.

14 B. Chu, *Science*, 2006, **313**, 334–336.

15 L. F. Malmonge and L. H. C. Mattoso, *Polymer*, 1995, **36**, 245–249.

16 A. J. Lovinger, *Science*, 1983, **220**, 1115–1121.

17 A. C. Jayasuriya and J. I. Scheinbeim, *Appl. Surf. Sci.*, 2001, **175–176**, 386–390.

18 M. Wegener, W. Kunstler, K. Richter, and R. Gerhard-Multhaupt, *J. Appl. Phys.*, 2002, **92**, 7442 –7447.

19 P. Kim, S. C. Jones, P. J. Hotchkiss, J. N. Haddock, B. Kippelen, S. R. Marder, and J. W. Perry, *Adv. Mater.*, 2007, **19**, 1001–1005.

20 Y. Rao and C. Wong, *J. Appl. Polym. Sci.*, 2004, **92**, 2228–2231.

21 T. J. Lewis, *J. Phys. Appl. Phys.*, 2005, **38**, 202–212.

22 H. T. Vo and F. G. Shi, *Microelectron. J.*, 2002, **33**, 409–415.

23 N. Joseph, S. K. Singh, R. K. Sirugudu, V. R. K. Murthy, S. Ananthakumar, and M. T. Sebastian, *Mater. Res. Bull.*, 2013, **48**, 1681–1687.

24 P. Thomas, K. T. Varughese, K. Dwarakanath, and K. B. R. Varma, *Compos. Sci. Technol.*, 2010, **70**, 539–545.

25 B. Shri Prakash and K. B. R. Varma, *Compos. Sci. Technol.*, 2007, **67**, 2363–2368.

26 Z.-M. Dang, T. Zhou, S.-H. Yao, J.-K. Yuan, J.-W. Zha, H.-T. Song, J.-Y. Li, Q. Chen, W.-T. Yang, and J. Bai, *Adv. Mater.*, 2009, **21**, 2077–2082.

27 M. Arbatti, X. Shan, and Z.-Y. Cheng, *Adv. Mater.*, 2007, **19**, 1369–1372.

28 F. Amaral, C. P. L. Rubinger, F. Henry, L. C. Costa, M. A. Valente, and A. Barros-Timmons, *J. Non-Cryst. Solids*, 2008, **354**, 5321–5322.

29 P. Thomas, K. Dwarakanath, and K. B. R. Varma, *Synth. Met.*, 2009, **159**, 2128–2134.

30 C. Yang, H. Song, and D. Liu, *Compos. Part B Eng.*, 2013, **50**, 180–186.

31 E. Tuncer, I. Sauers, D. R. James, A. R. Ellis, M. P. Paranthaman, T. Aytuğ, S. Sathyamurthy, K. L. More, J. Li, and A. Goyal, *Nanotechnology*, 2007, **18**, 025703.

32 X. Shan, L. Zhang, X. Yang, and Z.-Y. Cheng, *J. Adv. Ceram.*, 2012, **1**, 310–316.

33 P. Kim, N. M. Doss, J. P. Tillotson, P. J. Hotchkiss, M. J. Pan, S. R. Marder, J. Li, J. P. Calame, and J. W. Perry, *ACS Nano*, 2009, **3**, 2581–2592.

34 P. H. Mutin, G. Guerrero, and A. Vioux, *J Mater Chem*, 2005, **15**, 3761–3768.

35 T. Schulmeyer, S. A. Paniagua, P. A. Veneman, S. C. Jones, P. J. Hotchkiss, A. Mudalige, J. E. Pemberton, S. R. Marder, and N. R. Armstrong, *J. Mater. Chem.*, 2007, **17**, 4563–4570.

36 S. A. Paniagua, P. J. Hotchkiss, S. C. Jones, S. R. Marder, A. Mudalige, F. S. Marrikar, J. E. Pemberton, and N. R. Armstrong, *J. Phys. Chem. C*, 2008, **112**, 7809–7817.

37 Y. Shen, A. Gu, G. Liang, and L. Yuan, *Compos. Part Appl. Sci. Manuf.*, 2010, **41**, 1668–1676.

38 S. Siddabattuni, T. P. Schuman, and F. Dogan, *Mater. Sci. Eng. B*, 2011, **176**, 1422–1429.

39. W. Gao, L. Dickinson, C. Grozinger, F. G. Morin, and L. Reven, *Langmuir*, 1996, **12**, 6429–6435.

40 C. Ehrhardt, C. Fettkenhauer, J. Glenneberg, W. Münchgesang, C. Pientschke, T. Großmann, M. Zenkner, G. Wagner, H. S. Leipner, A. Buchsteiner, M. Diestelhorst, S. Lemm, H. Beige, and S. G. Ebbinghaus, *Mater. Sci. Eng. B*, 2013, **178**, 881–888.

41 S.-D. Cho and K.-W. Paik, in *Electronic Components and Technology Conference, 2001. Proceedings., 51st*, 2001, pp. 1418–1422.

42 D. Ma, T. A. Hugener, R. W. Siegel, A. Christerson, E. Mårtensson, C. Önneby, and L. S. Schadler, *Nanotechnology*, 2005, **16**, 724.

43 J. Liu, R. W. Smith, and W.-N. Mei, *Chem. Mater.*, 2007, **19**, 6020–6024.

44 A. K. Bhattacharya and G. Thyagarajan, *Chem. Rev.*, 1981, **81**, 415–430.

45 I. Gouzman, M. Dubey, M. D. Carolus, J. Schwartz, and S. L. Bernasek, *Surf. Sci.*, 2006, **600**, 773–781.
46 G. Guerrero, P. H. Mutin, and A. Vioux, *Chem. Mater.*, 2001, **13**, 4367–4373.
47 J. P. Calame, *J. Appl. Phys.*, 2006, **99**, 084101 –084101–11.
48 P. Thomas, *EXPRESS Polym. Lett.*, 2010, **4**, 632–643.

